

energy splitting of the 4E term deduced from the experimental datum for the rhombicity parameter E matches roughly the value of the corresponding orbital-level splitting calculated for the ferrous complex.

Acknowledgment. This work was supported by the Deutsche Forschungsgemeinschaft and the Centre National de la Recherche Scientifique (URA 424). R.W. thanks the Alexander von Humboldt Foundation for financial support.

Supplementary Material Available: Table S1, giving thermal parameters of anisotropic atoms, Table S2, giving hydrogen atom positional and thermal equivalent parameters, Table S3, giving a complete set of bond distances, Table S4, giving a complete set of bond angles, Table S6, giving positional parameters and their esd's for $[\text{NaC}222]^+$ and the $\text{C}_6\text{H}_5\text{Cl}$ solvate molecule, and Figure S1, showing a stereoview of the packing in the crystals of $[\text{Fe}(\text{CH}_3\text{CO}_2)\text{TPpivP}]^-\text{[NaC}222]^+\cdot\text{C}_6\text{H}_5\text{Cl}$ (20 pages); Table S5, giving observed and calculated structure factor amplitudes ($\times 10$) for all observed reflections (28 pages). Ordering information is given on any current masthead page.

Contribution from the Institut für Anorganische Chemie, Universität Regensburg, Universitätsstrasse 31, W-8400 Regensburg, Germany, and Department of Chemistry, University of Texas, Austin, Texas 78712-1167

Spectroscopic Studies of Zinc Benzenethiolate Complexes: Electron Transfer to Methyl Viologen

Thomas Türk,[†] Ute Resch,[‡] Marye Anne Fox,^{*‡} and Arnd Vogler^{*‡}

Received August 12, 1991

Mononuclear and tetranuclear zinc benzenethiolate complexes are studied by both spectroscopic and electrochemical methods. $\text{Zn}(\text{SPh})_4^{2-}$ and $\text{Zn}_4(\text{SPh})_{10}^{2-}$ represent tetrahedral fragments of the cubic zinc sulfide lattice. The structured absorption spectra of the zinc benzenethiolate complexes are ascribed to intraligand transitions for the mononuclear complex and to a composite of both intraligand and ligand-to-metal charge-transfer (LMCT) transitions for the tetranuclear species. The mononuclear complex does not emit, while the tetranuclear compound displays a short-lived metal-to-ligand charge-transfer (MLCT) emission. Photodegradation of both zinc complexes yields thianthrene, dibenzothiophene, and benzenethiol. $\text{Zn}_4(\text{SPh})_{10}^{2-}$ forms a ground-state charge-transfer complex with the dicationic electron acceptor methyl viologen in CH_3CN . Excitation of the charge-transfer absorption band with a 30-ps laser pulse leads to the formation of the methyl viologen radical cation showing a lifetime of 2 ± 0.4 ns.

Introduction

The chemistry of group IIb metal thiolate coordination is vital to an understanding of the interactions of these metals in biological systems.¹ Zinc and cadmium thiolate complexes² have been used as models for thiolate metalloproteins such as metallothioneins,³ which are located in the kidney and liver in a wide variety of animals, including man. These proteins bind various metallic cations such as zinc, cadmium, mercury, and copper through thiolate ligands and regulate the levels of these heavy metals in the organism.⁴

Native metallothioneins³ usually contain six or seven zinc or cadmium atoms bound to all 20 cysteine residues (via mercaptide linkages) in a single polypeptide chain of 61 total amino acid residues.⁴ Each zinc or cadmium atom is coordinated by four cysteine thiolate ligands as deduced from ^{113}Cd NMR studies.⁵ Spectroscopic studies of $\text{Co}(\text{II})$ -⁶ and $\text{Ni}(\text{II})$ -substituted⁷ metallothioneins also indicate tetrahedral $\text{M}(\text{Cys-S})_4$ sites. This tetrahedral coordination requires at least some bridging of the metal ions by cysteine sulfur and suggests that metal-cysteine adamantane-type complexes may be formed in these proteins.^{2b,5d}

Furthermore, short chelating peptides containing cysteine units have been used to synthesize near monodisperse nanometer-scale II-VI semiconductor crystallites⁸ exhibiting size-dependent and discrete excited electronic states that occur at energies higher than the band gap of the corresponding bulk semiconductor.⁹⁻¹² Semiconductor crystallites in the nanometer range (which still show the same crystal structure as the bulk material but are too small to have continuous energy bands) are currently under intense investigation in order to observe the photophysical properties of particles in the quantum-size region (size quantization effect).⁹⁻¹² A further reduction of the particle size yields molecular dimensions exhibiting typical properties such as structured absorption and emission spectra as well as structural rearrangements in the excited state.

In this paper, we report a detailed study of the photophysical and electrochemical behavior of a mononuclear ($\text{Zn}(\text{SPh})_4^{2-}$) and a tetranuclear ($\text{Zn}_4(\text{SPh})_{10}^{2-}$) zinc benzenethiolate complex. The synthesis and crystal structures of these zinc benzenethiolate complexes have been previously described.¹³⁻¹⁵ These tetrahedral

- (1) (a) Carty, A. J. *ACS Symp. Ser.* **1978**, *82*, 327-353.
- (2) (a) Swenson, D.; Baenziger, N. C.; Coucouvanis, D. J. *Am. Chem. Soc.* **1978**, *100*, 1932-1934. (b) Dance, I. G. *J. Am. Chem. Soc.* **1980**, *102*, 3445-3451. (c) Hagen, K. S.; Stephan, D. W.; Holm, R. H. *Inorg. Chem.* **1982**, *21*, 3928-3936. (d) Lacelle, S.; Stevens, W. C.; Kurtz, D. M.; Richardson, J. W.; Jacobson, R. A. *Inorg. Chem.* **1984**, *23*, 930-935. (e) Dance, I. G. *Inorg. Chim. Acta* **1985**, *108*, 227-230. (f) Dance, I. G. *Aust. J. Chem.* **1985**, *38*, 1745-1755.
- (3) Kaegi, J. H. R.; Nordberg, M., Eds. *Metallothionein*; Birkhauser Verlag: Basel, Switzerland, 1979; pp 41-122.
- (4) (a) Kaegi, J. H. R.; Himmelhoch, S. R.; Whanger, P. D.; Bethune, J. L.; Vallee, B. L. *J. Biol. Chem.* **1974**, *249*, 3537-3542. (b) Kojima, Y.; Berger, C.; Vallee, B. L.; Kaegi, J. H. R. *Proc. Natl. Acad. Sci. U.S.A.* **1976**, *73*, 3413-3417.
- (5) (a) Otvos, J. D.; Armitage, I. M. *J. Am. Chem. Soc.* **1979**, *101*, 7734-7736. (b) Otvos, J. D.; Armitage, I. M. *Proc. Natl. Acad. Sci. U.S.A.* **1980**, *77*, 7094-7098. (c) Otvos, J. D.; Olafson, R. W.; Armitage, I. M. *J. Biol. Chem.* **1982**, *257*, 2427-2431. (d) Boulanger, Y.; Goodman, C. M.; Forte, C. P.; Fesik, S. W.; Armitage, I. M. *Proc. Natl. Acad. Sci. U.S.A.* **1983**, *80*, 1501-1505.
- (6) (a) Vasak, M. *J. Am. Chem. Soc.* **1980**, *102*, 3953-3955. (b) Vasak, M.; Kaegi, J. H. R. *Proc. Natl. Acad. Sci. U.S.A.* **1981**, *78*, 6709-6713.
- (7) Vasak, M.; Kaegi, J. H. R.; Holmquist, B.; Vallee, B. L. *Biochemistry* **1981**, *20*, 6659-6664.
- (8) Dameron, C. T.; Reese, R. N.; Mehra, R. K.; Kortan, A. R.; Carroll, P. J.; Steigerwald, M. L.; Brus, L. E.; Winge, D. R. *Nature* **1989**, *338*, 596-597.
- (9) (a) Henglein, A. *Top. Curr. Chem.* **1988**, *143*, 113-180. (b) Henglein, A. *Chem. Rev.* **1989**, *89*, 1861-1873.
- (10) (a) Brus, L. E. *J. Phys. Chem.* **1986**, *90*, 2555-2560. (b) Steigerwald, M. L.; Brus, L. E. *Acc. Chem. Res.* **1990**, *23*, 183-188.
- (11) Wang, Y.; Herron, N. *J. Phys. Chem.* **1991**, *95*, 525-532.
- (12) Stucky, G. D.; MacDougall, J. E. *Science* **1990**, *47*, 669-678.
- (13) (a) Choy, A.; Craig, D.; Dance, I. G.; Scudder, M. J. *Chem. Soc., Chem. Commun.* **1982**, 1246-1247. (b) Dance, I. G.; Choy, A.; Scudder, M. L. *J. Am. Chem. Soc.* **1984**, *106*, 6285-6295.
- (14) Hencher, J. L.; Khan, M. A.; Said, F. F.; Tuck, D. G. *Polyhedron* **1985**, *4*, 1263-1267.
- (15) Hagen, K. S.; Holm, R. H. *Inorg. Chem.* **1983**, *22*, 3171-3174.

[†] Universität Regensburg.

[‡] University of Texas.

zinc benzenethiolate complexes show structural similarities both to metallothionein proteins (the spatial demands of cysteine and the phenyl group of benzenethiolate are comparable)^{2b} and to the semiconductor ZnS, having a zinc blende structure: all these systems consist of four-coordinate zinc surrounded by a tetrahedron of sulfur atoms.¹³⁻¹⁵ The optical, photochemical, and electrochemical properties of these zinc benzenethiolate complexes in CH₃CN are characterized and compared to those of the corresponding cadmium and mercury benzenethiolate complexes. Furthermore, electron transfer from the tetranuclear zinc complex to methyl viologen is studied by picosecond absorption spectroscopy.

Experimental Section

Materials. Benzenethiol, zinc nitrate tetrahydrate, triethylamine, tributylamine, tetramethylammonium chloride, tetrabutylammonium hexafluorophosphate, methyl viologen dichloride hydrate, thianthrene, and dibenzothiophene were used as received from Aldrich. All photochemical studies were carried out with spectroscopic grade solvents. The zinc benzenethiolate complexes were synthesized by following the procedure of Dance et al.¹³ and characterized by elemental analysis and FTIR spectroscopy. While solutions of the mononuclear complex underwent a slow thermal decomposition, the tetranuclear cluster was stable even in the presence of air for extended periods. Methyl viologen was used as the perfluorophosphate salt.

Methods. Absorption spectra were measured on a Hewlett-Packard 8451 A single-beam spectrophotometer. Beer's law was found to be satisfied at different concentrations. Steady-state luminescence spectra of the aerated Zn₄(SPh)₁₀²⁻ solutions in CH₃CN were recorded on an SLM Aminco 500C spectrofluorometer. The luminescence quantum yield of Zn₄(SPh)₁₀²⁻ was determined relative to tryptophan;¹⁶ excitation was at 290 nm. For the luminescence quantum yield of Zn₄(SPh)₁₀²⁻, a deviation of 10% is assumed. Photolyses of the zinc benzenethiolate complexes in CH₃CN were carried out with a 1000-W high-pressure mercury lamp. The lamp intensity was attenuated by using calibrated metal screens. High-resolution mass spectra (EI) were recorded on a VG Analytical mass spectrometer (ZAB 2-E). The oxidation and reduction peak potentials of the zinc benzenethiolate complexes in CH₃CN were determined by cyclic voltammetry as previously described for analogous cadmium benzenethiolate complexes.¹⁷ For the cyclic voltammetry, a conventional single-compartment electrochemical cell equipped with either a Pt-disk (oxidation) or a hanging-mercury-drop electrode (HMDE) (reduction) working electrode, a Pt-wire counter electrode, and a Ag/AgCl reference electrode was used.¹⁷

Time-resolved emission measurements with Zn₄(SPh)₁₀²⁻ in CH₃CN were performed by the method of time-correlated single-photon counting (SPC) using a mode-locked frequency-doubled Nd:YAG laser (Quantronix model 416) synchronously pumping a cavity-dumped dye laser (Coherent Model 701-3D; Rhodamine 6G). The dye laser output (at 586 nm) was frequency-doubled using an angle-tuned KDP crystal to produce pulses at 293 nm. The instrument response function was ca. 70 ps fwhm (full width at half-height of the maximum). The decay profiles were fit to a multiexponential decay function using standard least-squares deconvolution techniques. The shortest lifetime which could be determined was 25 ps. The quality of the fits was evaluated by the χ^2 test and from the randomness of the distribution of the residuals. The emission of Zn₄(SPh)₁₀²⁻ in air-saturated solution (CH₃CN) was monitored at 350 nm. An average deviation of $\pm 5\%$ was observed for the luminescence lifetime.

Absorption measurements on a subnanosecond time scale were performed using a pulse-probe method as previously described.¹⁸ The excitation source was a 30-ps pulse from a Quantel YG402 mode-locked Nd:YAG laser. After part of the laser fundamental was converted to the second harmonic (532 nm), the residual 1064-nm laser light was focused through a cell containing a continuum-generating medium (deuterated phosphoric acid in D₂O) to produce a pulse of coherent white light with a time profile the same as that of the laser. This white light was used as the analyzing beam and, after passing through the sample, was focused onto a spectrograph, where its entire spectrum could be recorded. The time profiles of the absorption spectra were acquired by repeatedly changing the path length of the analyzing beam. The available wavelength region was 380–750 nm; the time window was 30 ps–6 ns. The time resolution was limited by the width of the laser pulse. All experi-

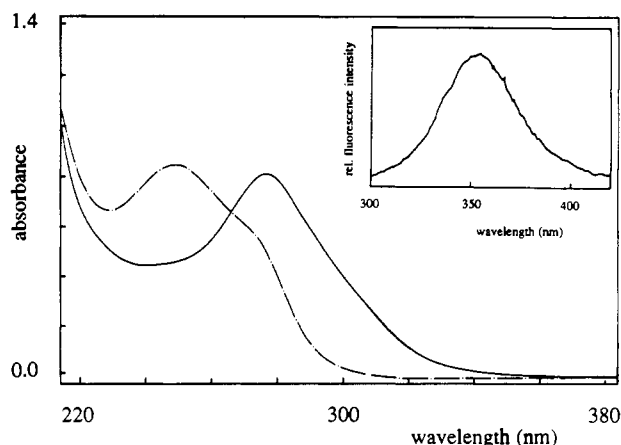


Figure 1. Absorption spectra of (—) 2.4×10^{-5} M Zn(SPh)₄²⁻ and (---) 1.2×10^{-5} M Zn₄(SPh)₁₀²⁻ in aerated CH₃CN. Inset: uncorrected emission spectrum of Zn₄(SPh)₁₀²⁻ in aerated CH₃CN, both at room temperature (1-cm cell; excitation at 310 nm).

ments were carried out in aerated CH₃CN at an optical density of 0.35 at 532 nm.

Results and Discussion

Absorption Spectra of Zn(SPh)₄²⁻ and Zn₄(SPh)₁₀²⁻. Figure 1 shows the absorption spectra of Zn(SPh)₄²⁻ and Zn₄(SPh)₁₀²⁻ in CH₃CN. Zn(SPh)₄²⁻, which contains only terminal ligands, displays one absorption band at 273 nm ($\epsilon_{273} = 33\,300$ M⁻¹ cm⁻¹), whereas Zn₄(SPh)₁₀²⁻, consisting of both terminal and bridging ligands, exhibits two absorption maxima at 250 nm ($\epsilon_{250} = 76\,300$ M⁻¹ cm⁻¹) and 270 nm ($\epsilon_{270} = 52\,600$ M⁻¹ cm⁻¹), respectively. The corresponding mono- and tetranuclear cadmium benzenethiolate complexes display similar spectra.¹⁷ The absorption spectrum of the ligand itself, benzenethiolate, is characterized by an absorption band located at 303 nm ($\epsilon_{303} = 13\,600$ M⁻¹ cm⁻¹).¹⁹

For Zn(SPh)₄²⁻, the absorption band at 273 nm is assigned to an intraligand transition, as related mononuclear zinc complexes (ZnL₂²⁻ with L = halide or OH⁻) do not show ligand-to-metal charge-transfer (LMCT) bands above 200 nm.^{20,21} Furthermore, the absorption spectrum of a Zn(SR)₄²⁻ complex with R = 2-PhC₆H₄ was assigned to pure intraligand transitions, as published recently.²² For the zinc benzenethiolate complexes reported here, a LMCT transition supposedly occurs from the filled 3p orbitals of the benzenethiolate sulfur (HOMO) to the empty 4s orbital located at Zn²⁺ (LUMO).²¹ For mononuclear tetrahedral Zn(II) complexes, the energy of the Zn²⁺ 4s orbital, which is the acceptor orbital of a LMCT transition, is apparently too high.²¹ In contrast to the mononuclear zinc complexes, related mononuclear cadmium thiolates show LMCT transitions in the 240–290-nm region,²³ as the Cd²⁺ 5s orbital is ca. 1.9 eV lower in energy than the Zn²⁺ 4s orbital.²⁴ Thus, for Zn(SPh)₄²⁻, the absorption bands are assigned to intraligand transitions, whereas the absorption spectrum of Cd(SPh)₄²⁻ is ascribed to a composite of intraligand and LMCT transitions.¹⁷

The absorption spectrum of Zn₄(SPh)₁₀²⁻ seems also to consist of intraligand bands. However, in contrast to the spectrum of the mononuclear complex, LMCT bands are assumed to contribute to the long-wavelength absorptions. This is not only concluded from the emission behavior of the cluster, which is different from that of Zn(SPh)₄²⁻, but is also supported by other arguments. Furthermore, the absorption spectrum of a related tetranuclear

(16) Miller, J. N., Ed. *Standards in Fluorescence Spectrometry*; Chapman and Hall: London/New York, 1981; pp 68–79.

(17) Türk, T.; Resch, U.; Fox, M. A.; Vogler, A. *J. Phys. Chem.*, in press.

(18) Atherton, S. J.; Hubig, S. M.; Callan, T. J.; Duncanson, J. A.; Snowden, P. T.; Rodgers, M. A. *J. Phys. Chem.* **1987**, *91*, 3137–3140.

(19) Thiophenolate is obtained by deprotonation of benzenethiol with sodium hydroxide in CH₃CN under N₂.

(20) Bird, B. D.; Day, P. *Chem. Commun.* **1967**, 741–745.

(21) Kunkely, H.; Vogler, A. *J. Chem. Soc., Chem. Commun.* **1990**, 1204–1205.

(22) Gebhard, M. S.; Koch, S. A.; Millar, M.; Devlin, F. J.; Stephens, P. J.; Solomon, E. I. *J. Am. Chem. Soc.* **1991**, *113*, 1640–1649.

(23) Carson, C. K.; Dean, P. A. W.; Stillman, M. J. *Inorg. Chim. Acta* **1981**, *56*, 59–71.

(24) Moore, C. E. *Atomic Energy Levels*; 1971; Vol. II, pp 128–129; Vol. III, pp 60–61.

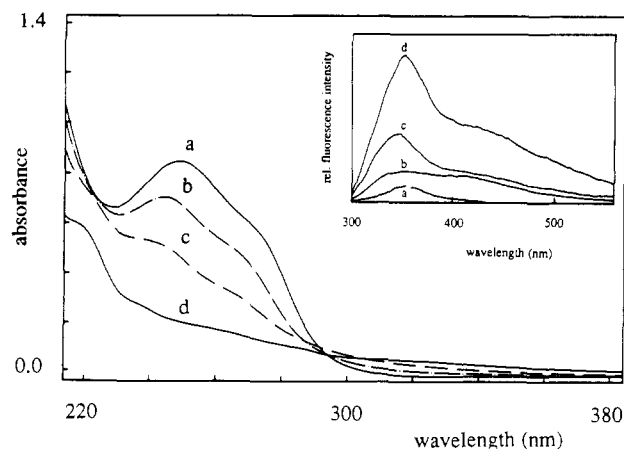


Figure 2. Photolysis of 1.2×10^{-5} M $\text{Zn}_4(\text{SPh})_{10}^{2-}$ in aerated CH_3CN . The absorption spectra were obtained after different illumination times: (a) before photolysis; (b) after 2 min; (c) after 5 min; (d) after 60 min. The inset shows the corresponding uncorrected emission spectra: (a) before photolysis ($\times 9$); (b) after 2 min ($\times 5$); (c) after 5 min ($\times 2$); (d) after 60 min. Excitation was always at 290 nm.

zinc-oxo complex, $\text{Zn}_4\text{O}(\text{acetate})_6$, shows a LMCT transition at 216 nm and a corresponding MLCT emission at 372 nm.²¹ As the number of the interacting sulfide and Zn^{2+} orbitals increases, a decrease in the energy of the LMCT transition is expected.^{11,21,25,26} Evidence for this behavior is provided by the photophysical properties of the related polynuclear cadmium benzenethiolate complexes, which display a bathochromic shift of the absorption onset with increasing complex size.^{11,17,26} The lower limit for this decrease in energy with increasing complex size is given by the band gap transition of bulk ZnS (onset of absorption, $\lambda_{\text{os}} = 335$ nm),²⁷ which can be considered a LMCT transition, since the valence band of ZnS is formed by filled 3p valence orbitals of sulfide whereas the conduction band is composed of empty Zn^{2+} 4s orbitals.^{21,25}

Luminescence Spectrum and Lifetime of $\text{Zn}_4(\text{SPh})_{10}^{2-}$. Both aerated and deaerated solutions of $\text{Zn}_4(\text{SPh})_{10}^{2-}$ in CH_3CN show a weak luminescence at 360 nm (inset of Figure 1). The quantum yield of this emission is determined to 3×10^{-3} . $\text{Zn}(\text{SPh})_4^{2-}$ displays no detectable emission. The latter result is in agreement with the literature, where no MLCT emission of mononuclear Zn^{2+} complexes has yet been reported.²¹

The luminescence of tetranuclear $\text{Zn}_4(\text{SPh})_{10}^{2-}$ is assigned to an (allowed) MLCT transition. An intraligand assignment is less likely, since the free ligand does not fluoresce at room temperature. The emission is Stokes-shifted from the absorption band at 270 nm by 9529 cm^{-1} . A considerable excited-state distortion is expected to be responsible for this Stokes shift, as the LMCT transition leads to the population of metal orbitals with bonding character.²⁸ The excitation spectrum of $\text{Zn}_4(\text{SPh})_{10}^{2-}$ does not follow the absorption spectrum of the complex, displaying only a band at 270 nm. This suggests that the absorption band at 250 nm has less LMCT character. There is apparently a restricted communication between intraligand and charge-transfer states.

A comparison of the luminescence properties of $\text{Zn}_4(\text{SPh})_{10}^{2-}$ with those of the analogous tetranuclear cadmium and mercury species,^{17,29} $\text{Cd}_4(\text{SPh})_{10}^{2-}$ and $\text{Hg}_4(\text{SPh})_6(\text{PPh}_3)_4^{2+}$, provides further information about the nature of the optical transitions involved: the emissions of zinc and cadmium complexes at 360 and 500 nm, respectively, are assigned to MLCT transitions,¹⁷ whereas the 690-nm emission of the mercury complex is ascribed to a mixture of MLCT and metal-centered $s \rightarrow d$ transition.²⁹ A red shift of

the MLCT emissions is expected as the energy of the ns metal orbitals decreases continuously from Zn^{2+} 4s via Cd^{2+} 5s to Hg^{2+} 6s.²⁴

Photodecomposition of $\text{Zn}(\text{SPh})_4^{2-}$ and $\text{Zn}_4(\text{SPh})_{10}^{2-}$. Illumination of $\text{Zn}_4(\text{SPh})_{10}^{2-}$ leads to a strong decrease of the absorption bands with time (Figure 2). Concomitantly, the emission of the complex at 360 nm disappears and a new broad luminescence band with a maximum at 355 nm and a shoulder at 440 nm is observed (inset of Figure 2). $\text{Zn}(\text{SPh})_4^{2-}$ shows a similar photochemical behavior, but it decomposes ca. 10 times faster than $\text{Zn}_4(\text{SPh})_{10}^{2-}$.³⁰ An explanation for the increasing stability from the mononuclear to the tetranuclear complex is, presumably, the increasing electronic delocalization, which makes bond cleavages within the tetranuclear species less likely. The photodecompositions of both zinc benzenethiolate complexes, which are unaffected by oxygen, most likely yield the same photoproducts, as suggested by the identical absorption and luminescence spectra observed at long illumination times.

Analysis of the illuminated zinc benzenethiolate solutions by mass spectroscopy suggests the formation of thianthrene, dibenzothiophene, and benzenethiol as photoproducts.¹⁷ Furthermore, a superposition of both the absorption and the emission spectra of these compounds seemingly fits the absorption spectrum (Figure 2, spectrum d) and emission spectrum (inset of Figure 2, spectrum d) of the photolyzed zinc benzenethiolate complexes. The fact that none of these photoproducts contain oxygen is consistent with the insensitivity of the photodecomposition of the zinc benzenethiolate complexes to oxygen. A solid residue of the photolyzed solutions was analyzed for ZnO and ZnS by ESCA spectroscopy. Neither possible product was detected. The very short luminescence lifetime of $\text{Zn}_4(\text{SPh})_{10}^{2-}$ makes a bimolecular photoreaction with O_2 impossible. Similar results are obtained for the corresponding Cd compounds.¹⁷

Electrochemical Study of $\text{Zn}(\text{SPh})_4^{2-}$ and $\text{Zn}_4(\text{SPh})_{10}^{2-}$. Cyclic voltammetry was carried out with deaerated solutions of both $\text{Zn}(\text{SPh})_4^{2-}$ and $\text{Zn}_4(\text{SPh})_{10}^{2-}$ in CH_3CN in order to determine their redox potentials. The oxidation of the zinc benzenethiolate complexes is presumably sulfur-centered, and the reduction, metal-centered.^{31,32} $\text{Zn}(\text{SPh})_4^{2-}$ and $\text{Zn}_4(\text{SPh})_{10}^{2-}$ display broad oxidation waves at 1.08 and 0.79 V vs Ag/AgCl, respectively,³³ which are both chemically irreversible at all scan rates up to 200 V s^{-1} . The position of the oxidation peak potential is seemingly affected by the complex size; i.e., with increasing complex size, the oxidation peak potential is shifted to less positive values. A similar dependence of the oxidation peak potential on complex size is observed for the corresponding cadmium benzenethiolate complexes.¹⁷ With increasing complex size, the LUMO centered at the metal is shifted to lower, and the HOMO located at the sulfur ligands is shifted to higher, energies.

Neither $\text{Zn}(\text{SPh})_4^{2-}$ nor $\text{Zn}_4(\text{SPh})_{10}^{2-}$ displays reduction waves at potentials less negative than -2.8 V vs Ag/AgCl. A similar behavior is observed for the corresponding mononuclear cadmium benzenethiolate complex, but the tetranuclear cadmium species shows a reduction wave at -2.47 V vs Ag/AgCl. The fact that the reduction of the zinc benzenethiolate complexes occurs at more negative potentials than that of the corresponding cadmium compounds is consistent with the fact that Cd^{2+} is reduced at less negative potentials than Zn^{2+} .³⁴

Electron Transfer to Methyl Viologen. Solutions of $\text{Zn}_4(\text{SPh})_{10}^{2-}$ (counterion: Me_4N^+) and methyl viologen, MV^{2+} (counterion: PF_6^-), exhibit absorption spectra typical of an ion-pair complex (Figure 3).³⁵ The broad charge-transfer absorption band which

(25) Bahnemann, D. W.; Kormann, C.; Hoffmann, M. R. *J. Phys. Chem.* **1987**, *91*, 3789–3798.

(26) Herron, N.; Wang, Y.; Eckert, H. *J. Am. Chem. Soc.* **1990**, *112*, 1322–1326.

(27) *Landolt-Bernstein*; Springer Verlag: Berlin/Heidelberg, 1982; Vol. 17b, p 61.

(28) Vogler, A.; Kunkely, H. *Chem. Phys. Lett.* **1989**, *158*, 74–76.

(29) Kunkely, H.; Vogler, A. *Chem. Phys. Lett.* **1989**, *164*, 621–624.

(30) The relative photodegradation rates are estimated from the illumination times required to decrease the absorption of the zinc benzenethiolate complexes by 50% at the same extinction.

(31) Baral, S.; Fojtik, A.; Weller, H.; Henglein, A. *J. Am. Chem. Soc.* **1986**, *108*, 375–378.

(32) Dunstan, D. E.; Hagfeldt, A.; Almgren, M.; Siegbahn, H. O. G.; Mukhtar, E. *J. Phys. Chem.* **1990**, *94*, 6797–6804.

(33) The oxidation peak potentials were determined at a scan rate of 200 mV s^{-1} .

(34) Atkins, P. W. *Physical Chemistry*, 3rd ed.; Freeman: New York, 1986; p 825.

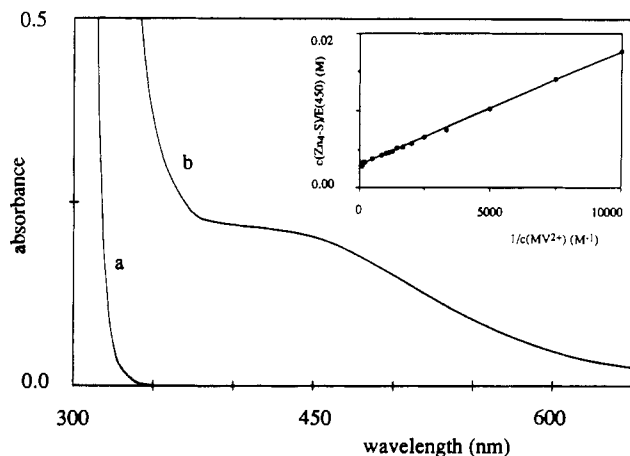


Figure 3. Charge transfer complex of $Zn_4(SPh)_{10}^{2-}$ (counter ion: Me_4N^+) with MV^{2+} (counter ion: PF_6^-) in aerated CH_3CN : (a) absorption spectrum of $Zn_4(SPh)_{10}^{2-}$ ($c(Zn_4(SPh)_{10}^{2-}) = 3.4 \times 10^{-4}$ M); (b) absorption spectrum of $Zn_4(SPh)_{10}^{2-}/MV^{2+}$ ($c(Zn_4(SPh)_{10}^{2-}) = 3.4 \times 10^{-4}$ M; $c(MV^{2+}) = 1.0 \times 10^{-2}$ M). Inset: Benesi-Hildebrand plot for $Zn_4(SPh)_{10}^{2-}$.

is not present in either $Zn_4(SPh)_{10}^{2-}$ or MV^{2+} alone is centered at 445 nm.³⁶ The complex formation equilibrium constant and the extinction coefficient (at 445 nm) of the 1:1 ground-state charge-transfer complex are determined to be 2000 ± 200 M⁻¹ and 340 M⁻¹ cm⁻¹, respectively, by applying the Benesi-Hildebrand method (inset of Figure 3).³⁷ The formation of a ground-state charge-transfer complex with MV^{2+} showing a similar absorption spectrum, but both a higher (by a factor of ca. 2) complex formation constant and extinction coefficient, is also observed for the corresponding tetranuclear cadmium benzenethiolate complex.¹⁷ For $Zn(SPh)_4^{2-}$, addition of MV^{2+} leads to the formation of the methyl viologen radical cation, $MV^{•+}$, either by thermal electron transfer or by reaction of the photoproduct with MV^{2+} .³⁸

The transient absorption spectrum of the $Zn_4(SPh)_{10}^{2-}/MV^{2+}$ charge-transfer complex, recorded immediately after the 30-ps laser pulse, shows the reduced methyl viologen, $MV^{•+}$, absorbing at 395 and 605 nm (Figure 4).³⁹ The absorption spectrum decays via first-order kinetics back to the baseline, as expected for an ion-pair which does not diffuse apart upon charge separation. From the decay at 605 nm, a lifetime of 2.0 ± 0.4 ns is determined for the methyl viologen radical cation (inset of Figure 4).

Conclusions

The optical, photochemical, and electrochemical properties of a mononuclear and a tetranuclear zinc benzenethiolate complex

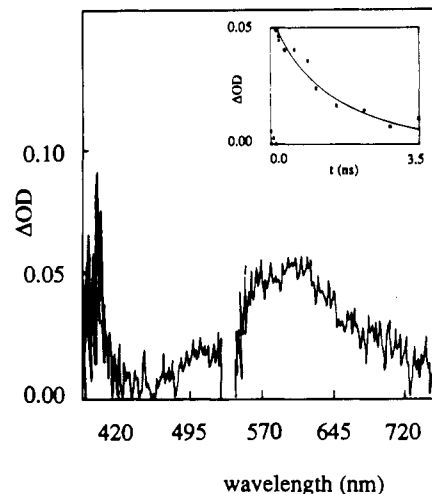


Figure 4. Transient absorption difference spectrum recorded immediately after excitation ($\lambda = 532$ nm) of $Zn_4(SPh)_{10}^{2-}$ in CH_3CN with a 30-ps laser pulse ($c(Zn_4(SPh)_{10}^{2-}) = 1.6 \times 10^{-3}$ M; $c(MV^{2+}) = 1.0 \times 10^{-1}$ M). Inset: absorbance decay profile at 605 nm. The decay profile was analyzed by first-order kinetics, giving a lifetime of 2.0 ± 0.4 ns for the reduced MV^{2+} .

are studied. Both $Zn(SPh)_4^{2-}$ and $Zn_4(SPh)_{10}^{2-}$ show structured absorption spectra which are assigned to intraligand transitions for the mononuclear complex. The absorption spectrum of the tetranuclear species is most likely a composite of both intraligand and ligand-to-metal charge-transfer (LMCT) transitions, as suggested by its excitation spectrum. The tetranuclear zinc complex displays a metal-to-ligand charge-transfer (MLCT) emission with a quantum yield of 3×10^{-3} and a lifetime of 35 ps. The mononuclear zinc complex does not emit. The photodegradation of both zinc complexes yields thianthrene, dibenzothiophene, and benzenethiol. Electrochemical studies of the zinc benzenethiolate complexes suggest size-dependent oxidation peak potentials: with increasing complex size, the oxidation wave is shifted to less positive values. For both complexes, no reduction waves are observed at potentials less negative than -2.8 V vs Ag/AgCl.

$Zn_4(SPh)_{10}^{2-}$ forms a 1:1 ground-state charge-transfer complex with the cationic electron acceptor methyl viologen. Excitation of the charge-transfer band of this complex with a 30-ps laser pulse leads to the formation of the reduced methyl viologen, which decays via first-order kinetics. The lifetime of the methyl viologen radical cation is determined to be 2.0 ± 0.4 ns.

Acknowledgment. We thank F. Sabin for help with the synthesis of the zinc benzenethiolate complexes, Dr. J. Merkert for assistance with the electrochemical measurements, D. J. Kiserow and Dr. S. J. Atherton for help with the time-resolved emission measurements, and Dr. S. M. Hubig for stimulating discussions. Financial support of the work at the University of Regensburg by the Deutsche Forschungsgemeinschaft and at the University of Texas by the U.S. Army Research Office is gratefully acknowledged. Initial SPC measurements were made at the Center for Fast Kinetics Research, a facility jointly supported by the National Institutes of Health and the University of Texas.

(35) Vogler, A.; Kunkely, H. *Top. Curr. Chem.* **1990**, *158*, 1-30.

(36) The exact positions of the maxima of the CT complexes are obtained from the second derivatives of the absorption spectra of $Zn_4(SPh)_{10}^{2-}/MV^{2+}$.

(37) (a) Benesi, H. A.; Hildebrand, J. H. *J. Am. Chem. Soc.* **1949**, *71*, 2703-2707. (b) Deranleau, D. A. *J. Am. Chem. Soc.* **1969**, *91*, 4044-4049.

(38) Henglein, A. *J. Phys. Chem.* **1982**, *86*, 2291-2293.

(39) Hubig, S. M.; Dionne, B. C.; Rodgers, M. A. *J. Phys. Chem.* **1986**, *90*, 5873-5876.